Article:

Gardner, L. J., Lejeune, V., Corkhill, C. L. et al. (2015) Evolution of phase assemblage of blended magnesium potassium phosphate cement binders at 200 degrees and 1000 degrees C. Advances in Applied Ceramics, 114 (7). pp. 386-392. ISSN: 1743-6753

https://doi.org/10.1179/1743676115Y.0000000064

Evolution of the phase assemblage of blended magnesium potassium phosphate cement binders at 200^{o}C and 1000^{o}C.

Laura J. Gardner[1], Valentin Lejeune[1,2], Claire L. Corkhill[1], Susan A. Bernal[1], John L. Provis[1] ,
M.C. Stennett,[1] and Neil C. Hyatt[1*]

[1]Immobilisation Science Laboratory, Department of Materials Science and Engineering, University of Sheffield, Sir Robert Hadfield Building, Portobello Street, Sheffield S1 3JD, UK

[2]École Nationale Supérieure de Chimie de Montpellier, 8 Rue de l'Ecole Normale, 34090, Montpellier, France

**To whom correspondence should be addressed. Email n.c.hyatt@sheffield.ac.uk, phone +44 (0) 114 222 5470, fax +44 (0) 114 222 5943*

ABSTRACT

The fire performance of magnesium potassium phosphate cement (MKPC) binders blended with fly ash (FA) and ground granulated blast furnace slag (GBFS) was investigated up to 1000 °C using XRD, TGA, and SEM techniques. The FA/MKPC and GBFS/MKPC binders dehydrate above 200 °C to form amorphous $KMgPO_4$, concurrent with volumetric and mass changes. Above 1000 °C, additional crystalline phases were formed and microstructural changes occurred, although no cracking or spalling of the samples was observed. These results indicate that FA/MKPC and GBFS/MKPC binders are expected to have satisfactory fire performance under the fire scenario conditions relevant to the operation of a UK or other geological disposal facility.

Key Words: MKPC, fly ash, ground granulated blast furnace slag, fire performance, nuclear waste

1. INTRODUCTION

Magnesium potassium phosphate cements (MKPCs) are a near-neutral pH system based on an acid-base reaction between MgO and KH_2PO_4, which form the main cementitious binder struvite-K ($MgKPO_4.6H_2O$). Their properties also include: low water demand, low drying shrinkage, and high early compressive strength [1], which has favoured application of MKPCs to radioactive waste encapsulation [2]. MKPCs have been extensively researched at the Argonne National Laboratory (ANL), USA, to encapsulate wastes that are not compatible with standard cementation (blended Portland cement) such as nitrated wastes and Pu contaminated materials[3-9]. In the UK, the near-neutral pH and low water demand properties of MKPCs are advantageous in the immobilisation of radioactive reactive metals (Al, Mg and U), which could otherwise corrode in the highly alkaline and/or high free water environment of Portland cement [2, 10-12].

UK nuclear wasteforms (waste and cement encapsulant) and waste packages (wasteform and container) have stringent safety requirements as laid out in the generic waste packaging specifications [13, 14] by Radioactive Waste Management Limited (RWM) based on the mechanical, immersion and thermal properties of waste packages. Taking the latter into consideration, all waste packages should be designed to minimise the release of radioactive materials whilst retaining wasteform integrity during exposure to a thermal excursion (i.e. a fire)[13] that could occur during interim storage, transportation or geological disposal.

There is a low fire risk associated with an underground repository, but nonetheless, such events do occur. For example, two fire incidents occurred in 2014 at the Waste Isolation Pilot Plant (WIPP), USA, resulting in Pu contamination in the underground ventilation system[15]. This highlights the need for detailed understanding of materials performance under fire conditions especially where access is limited, such as an underground repository where a fire could reach (and sustain) higher temperatures than an above-ground fire [13].

In general terms, exposure of cement-based structures to high temperature leads to severe deterioration and potential loss of mechanical strength. This is associated with several factors including: water evaporation increasing the pressure within pores; differences in the thermal expansion coefficients of the particles and gels present in the material causing cracking; and the transformations and dehydration reactions leading to the progressive breakdown of the binding gel [16, 17]. In the context of the storage and disposal of cement-based nuclear waste, determining the wasteform performance upon exposure to high temperatures is important to safeguard waste package integrity. Under such circumstances, an external fire could have severely detrimental effects, such as expansion leading to cracking and loss of the radioactive waste containment function.

It is anticipated that MKPCs can withstand high temperatures as magnesium phosphate compounds were historically used as castable refractory materials in the intermediate zone within high temperature furnaces[18-20], due to their ability to withstand a wide range of temperature conditions. In practical applications, including development as a matrix for nuclear waste encapsulation, MKPC binders are often blended (up to 50 wt. % replacement) with supplementary cementitious materials (SCMs) to reduce the exothermic output of the acid-base reaction, to reduce material costs [12] and to ensure sufficient workability. Therefore, it is important to understand the effect of high temperatures on these blended binders, relevant to fire scenarios in a geological disposal facility. In this study, MKPC blended with fly ash (FA/MKPC) and ground granulated blast furnace slag (GBFS/MKPC), was exposed to temperatures between 20 °C to 1000 °C and the products were characterised using X-ray diffraction (XRD), thermogravimetric analysis (TGA), and scanning electron microscopy (SEM) techniques, to assess their high temperature stability.

2. EXPERIMENTAL DESIGN

2.1 Materials

MKPC formulations utilised MgO (Richard Baker Harrison Ltd), in the form of dead burnt magnesite (DBM) (89% purity), KH_2PO_4 (Prayon UK) available as Food Grade E340 MKP (>99% purity) and granular boric acid (H_3BO_3) from Fisher Scientific UK (>99.5% purity). Fly ash (FA) was supplied by CEMEX as PFA BS EN 450-1 S. Ground granulated blast furnace slag (GBFS) from Scunthorpe Steelworks was supplied by Hanson Cement according to the established specifications of Sellafield Limited for use in the UK nuclear industry, and is a blend of finely-ground and coarser-ground materials. The chemical compositions of MgO, FA and GBFS were determined by X-ray fluorescence (XRF), Table 1.

Table 1. Composition of raw materials as determined by XRF oxide analysis (precision ± 0.1 wt. %).

Compound (wt. %)	MgO	FA	GBFS
Na_2O	<0.1	1.1	0.4
MgO	88.9	1.7	7.9
Al_2O_3	1.7	25.2	12.0
SiO_2	4.3	50.2	36.6
P_2O_5	<0.1	0.3	<0.1
K_2O	0.1	3.6	0.7
CaO	2.1	2.4	40.2
Fe_2O_3	1.5	9.3	0.4
Total	98.8	93.8	98.3

2.2 Mix design

The blended MKPC formulations were calculated based on a 1.7: 1 MgO: KH_2PO_4 molar ratio with a water-to-solids (w/s) ratio of 0.24 was used to produce the main binder phase, struvite-K, $MgKPO_4{\cdot}6H_2O$ (Eq. 1), with the addition of 50 wt. % of either FA or GBFS (as a diluent) and 2 wt. % H_3BO_3 (as a set retarder). The precursors (MgO, KH_2PO_4, FA or GBFS, H_2O, and H_3BO_3) were mixed initially for 10 minutes in a Kenwood mixer. Afterwards, the paste was transferred to a high shear Silverson mixer (4000 rpm) and mixed for an additional 10 minutes to achieve a homogenous paste. The binders were cured in an environmental chamber at 20 °C and 95 % relative humidity in sealed vessels for 7 days, prior to the thermal exposure and subsequent analysis. The formulations used in this study (Table 2) were based on previous research[21] where a low water-to-solids (w/s) ratio was required to reduce the inherent risk of corrosion (and consequent H_2 gas generation) in a wasteform comprised of metallic intermediate level waste streams (Mg, Al or U) during either interim storage or geological disposal [11].

$$MgO_{(s)} + KH_2PO_{4\,(s)} + H_2O_{(l)} \rightarrow MgKPO_4{\cdot}6H_2O_{(s)} \qquad \text{(Eq. 1)}$$

Table 2. Formulation of blended MKPC pastes produced with 0.24 water/solids ratio, based on a 200g batch size to ± 0.1 g precision.

Blend	MgO (g)	KH_2PO_4 (g)	H_2O (g)	FA (g)	GBFS (g)	H_3BO_3 (g)
FA/MKPC	31.1	61.8	38.4	66.1	-	2.6
GBFS/MKPC	31.1	61.8	38.4	-	66.1	2.6

2.3 Thermal test method

Blended MKPC samples (cured for 7 days) were cut into cylinders (*h* = 10 mm ± 0.1 mm and *d* = 14 mm ± 0.5 mm) using a Buehler Isomet low speed saw. The samples (on a zirconia tile) were placed into a pre-heated furnace (Elite; model 15/5) at 200 °C and 1000 °C, respectively. After allowing the furnace time to stabilise (<5 minutes) and the 30 minute exposure, the samples were removed and quenched to room temperature, as illustrated in Figure 1.

The thermal test methodology was based on a combination of the IAEA transport regulations [22] and the Radioactive Waste Management Limited (RWM) requirements for a geological disposal facility (GDF) in the UK [13]. The IAEA thermal test method involves samples to be fully engulfed with an average temperature of 800 °C (based on a hydrocarbon fuel fire with a flame emissivity coefficient of 0.9) for a 30 minute period [22], whereas the RWM parameters (as reported by Nuclear Decommissioning Authority (NDA)) increased the average temperature and duration to 1000 °C and 1 hour, respectively [13]. This is associated with a higher risk factor, as any fire in a GDF may reach higher temperatures, due to heat reflected off tunnel features, and for longer due to restricted access compared to an above-ground fire [13], so it is necessary that waste packages can withstand higher temperatures whilst retaining their integrity. However, due to the small sample size used in this study, the samples were exposed to elevated temperatures (200 °C and 1000 °C) for only 30 minutes rather than the 1 hour parameter suggested by RWM.

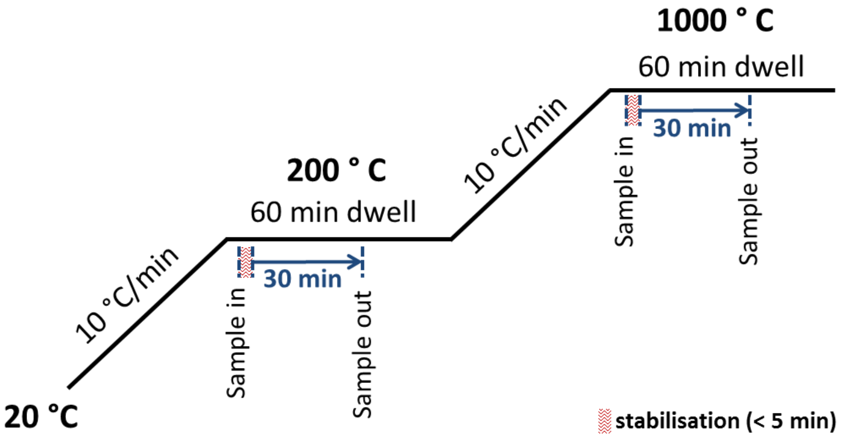

Fig. 1. The fire performance thermal treatment schedule

2.4 Analytical techniques

Powder X-ray diffraction (XRD) data were collected between 10° < 2θ < 50° using a Bruker D2 PHASER desktop diffractometer with a Cu Kα (1.5418 Å) source operating in reflection geometry, using a step size of 0.02° and time per step of 1 s. Thermogravimetric analysis (TGA) was conducted on samples after 7 days of curing using a Pyris 1 TGA instrument, with 20 mg of sample in an alumina crucible at a heating rate of 10 °C/min to 1000 °C in a nitrogen atmosphere. SCM-blended MKPC samples were polished and carbon coated for analysis using a Jeol JSM 6400 SEM at a 20 kV accelerating voltage and a working distance of 15 mm.

3. Results

3.1 Physical properties

Table 3 shows the volumetric and mass changes of FA/MKPC and GBFS/MKPC binders after exposure to 200 °C and 1000 °C. It was evident that a large mass loss event occurred in both binders below 200 °C, which resulted in a similar mass change of ≈ -21 % (Table 3). This was associated with the dehydration of the main binding phase struvite-K, $MgKPO_4 \cdot 6H_2O$, as evidenced in the subsequent sections. The relative volume of each specimen was observed to increase when heating from 200 °C to 1000 °C, which suggested that new or additional phases were formed as a result of chemical interactions within the binder.

Table 3. Volumetric and mass changes of blended MKPC samples after heating from 20 to 200 or 1000 °C, to ± 0.1 % precision.

		% change after heating	
Blend	**Temp (°C)**	**Mass (± 0.3 %*)**	**Volume (± 0.4 %*)**
FA/MKPC	200	-20.7	-6.1
	1000	-26.4	-4.2
GBFS/MKPC	200	-20.8	-8.8
	1000	-23.7	-3.4

* The errors are associated with calculated standard deviations from the 800 °C experiment carried out in triplicate (data not shown)*

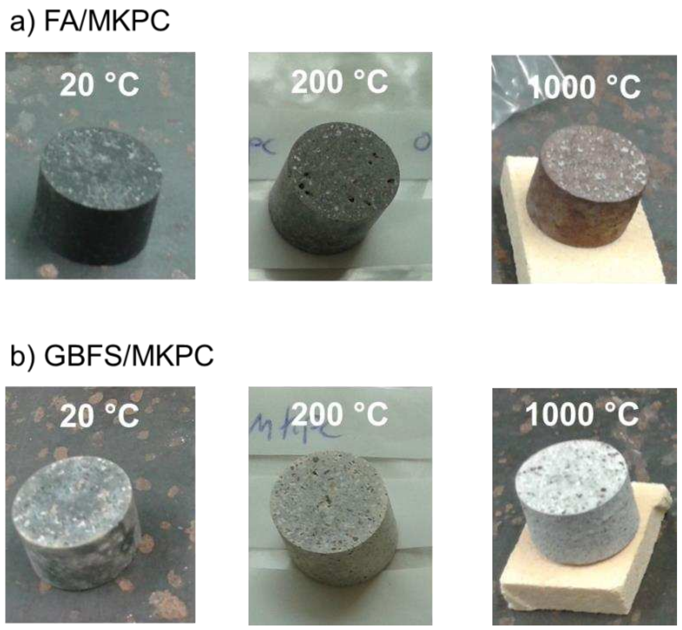

Fig. 2. Photographs of a) FA/MKPC and b) GBFS/MKPC hardened pastes exposed to temperatures of 20, 200 and 1000 °C. The samples are; 14 mm diameter (± 0.6 mm) and 10 mm height (± 0.5 mm).

It was evident in the collective photographs of the FA/MKPC and GBFS/MKPC binders (Fig. 2) that no spalling or cracking occurred after exposure to high temperatures. This suggests that blended MKPC binders are stable as they can tolerate dimensional changes (expansion and contraction), which liken them to the magnesium phosphate cement origins as refractory linings [19]. In the FA/MKPC binder (Fig. 2a), a colour change (from dark grey to red brown) was observed between the 20 °C and 1000 °C samples. This was associated with a change in Fe speciation, in favour of Fe(III), which was confirmed using ^{57}Fe Mössbauer spectroscopy (data not shown). However, in the GBFS/MKPC binder a more subtle colour change (from grey to light grey) was observed; this was possibly due to the lower combined Fe content (GBFS and MgO) than in FA/MKPC (1.9 wt. % compared with 9.7 wt. % for FA/MKPC, Table 1).

3.2 Thermogravimetric analysis

The dehydration behaviour of FA/MKPC and GBFS/MKPC binders as measured using TGA and derivative thermogravimetric (DTG) analysis, shown in Figure 3, was found to be comparable to that of pure struvite-K systems [23]. Significant mass changes occurred between 40 °C and 110 °C, which were calculated to be -18 % and -20 % for the two blends respectively. This was assigned to the single-step dehydration of $MgKPO_4 \cdot 6H_2O$, leading to the formation of the dehydrated phase $MgKPO_4$ (Eq. 2). There was a 2 % point difference between FA/MKPC and GBFS/MKPC, which suggested that more of the cementitious struvite-K phase was present in the GBFS/MKPC sample. The density of the GBFS used in this study was 2885 ± 5 kg/m^3, whilst the FA had a density of 2329 ± 5 kg/m^3. This density difference between the supplementary cementitious materials (SCMs) could also explain the disparity observed in Figure 3, as the slightly denser GBFS would occupy a smaller volumetric contribution (in a 20 mg TG sample) than the FA and, as such, it would appear that additional struvite-K had formed in the GBFS/MKPC binder. The authors have recently reported that FA and GBFS do not behave as inert fillers within the MKPC system but rather that incongruent dissolution results in the formation of secondary reaction products [24], which makes it difficult to accurately quantify the proportion of the volumetric composition.

The DTG analysis shown in Figure 3b further emphasises that only one mass loss event occurred. The TGA and DTG results did not identify any other significant weight loss events in either binder, suggesting that the inclusion of FA and GBFS within MKPC binders does not have an effect on the dehydration behaviour.

$$MgKPO_4 \cdot 6H_2O_{(s)} \rightarrow MgKPO_4 + 6H_2O_{(g)} \qquad \text{(Eq. 2)}$$

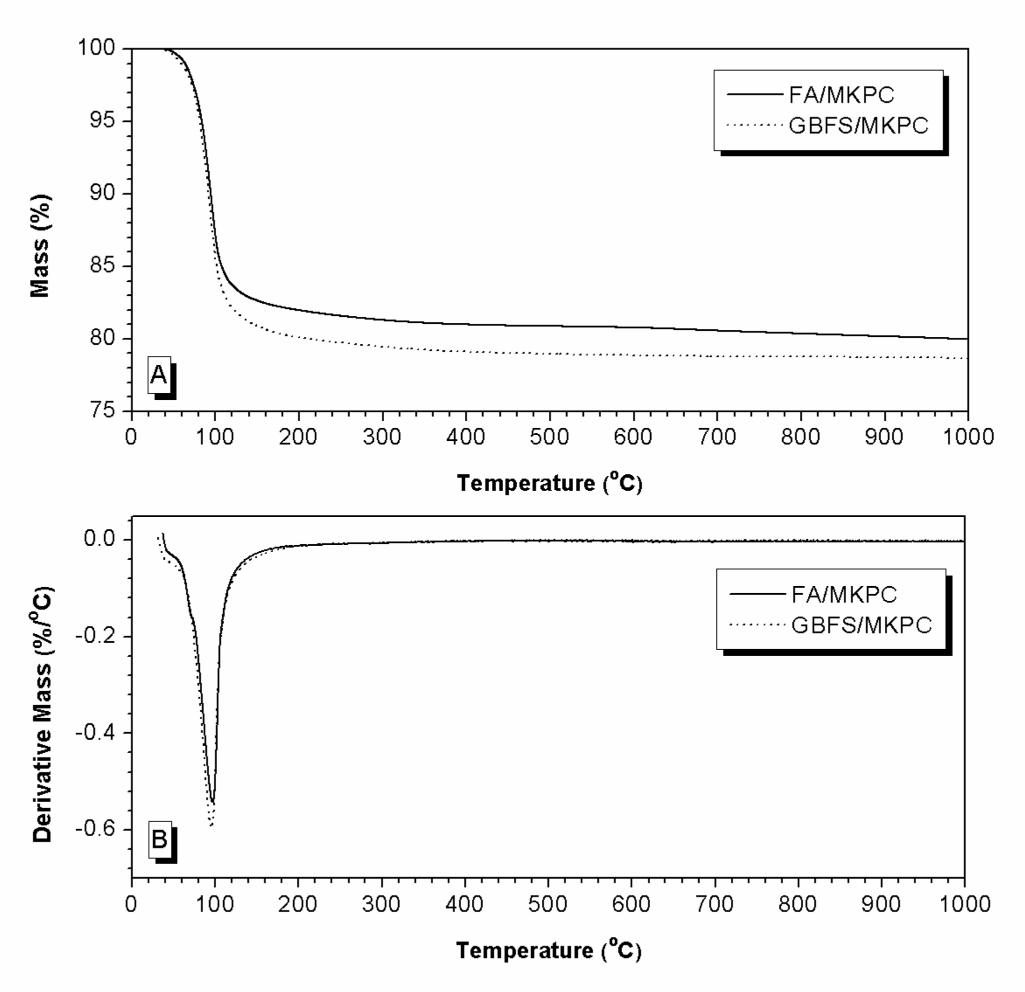

Fig. 3. a) TGA and b) DTG data for FA/MKPC and GBFS/MKPC pastes after 7 days curing.

3.3. Powder X-ray diffraction

3.3.1 FA/MKPC

X-ray diffraction (XRD) was utilised to observe the mineralogical changes in blended MKPC binders exposed to high temperatures (200 °C and 1000 °C). At 20 °C, struvite-K ($MgKPO_4·6H_2O$, powder diffraction file (PDF) #75-1076) was identified as the main crystalline product formed in the FA/MKPC binder (Fig. 4). Traces of unreacted periclase (MgO, PDF #45-0946), and crystalline quartz (SiO_2, PDF #78-2315 and mullite ($Al_6Si_2O_{13}$, PDF #15-0776) from the unreacted FA were also identified.

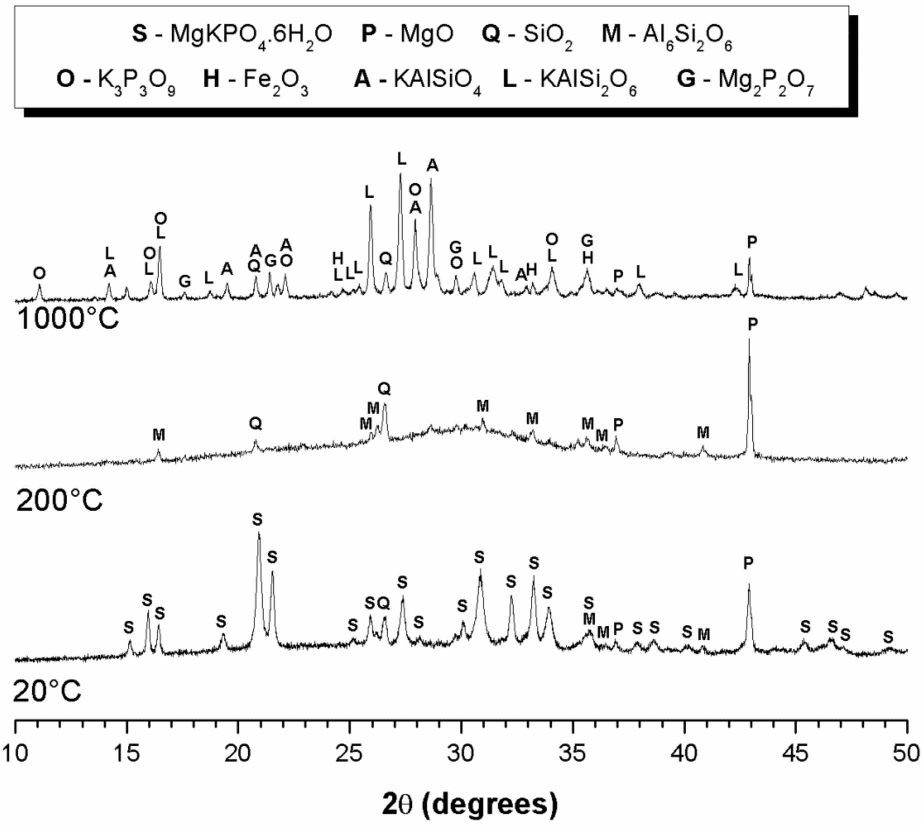

Fig. 4. X-ray diffraction patterns of FA/MKPC pastes exposed to temperatures of 20, 200 and 1000 °C.

After exposing the FA/MKPC binder to 200 °C, the reflections for periclase, quartz and mullite remained unchanged whereas the struvite-K reflections were absent. This was associated with dehydration of struvite-K to a $KMgPO_4$ phase, as observed in the TGA/DTG (Fig. 3); however, no reflections were observed for a newly formed crystalline phase at this exposure temperature, which suggests that the $MgKPO_4 \cdot 6H_2O$ collapsed to a non-crystalline phase upon dehydration. This is supported by previous investigation of struvite ($NH_4MgPO_4.6H_2O$); it was established that no reflections for the equivalent dehydrated phase were identified between 200 °C – 700 °C for this phase [25-27]. Neiman and Sarma [25] postulated that this was due to the formation of a non-crystalline polymeric phase, whereas Sarkar [26] suggested that $MgHPO_4$ was formed due to liberation of both the crystal-bound H_2O and NH_4, that occurred because struvite is unstable above 50 °C. In contrast, Abdelrazig and Sharp [27] suggested that a glassy material observed between $17° < 2\theta \leq 34°$ could be assigned to the $NH_4H_2PO_4$ phase. Although these interpretations vary, it is clear that the dehydrated struvite (and thus, conceivably also the isostructural struvite-K [28, 29]) has no long-range order until ≥ 700 °C. In Figure 3, diffuse scattering was identified between $15° < 2\theta \leq 40°$; typically diffuse scattering associated with the glassy FA fraction is assigned between $15° < 2\theta \leq 25°$, it is therefore postulated that non-crystalline $KMgPO_4$ also contributes to the diffuse scattering from materials annealed at 200 °C.

At 1000 °C, the conversion of Al, Si (present in FA) and K to a potassium aluminosilicate phases, kalsilite ($KAlSiO_4$, PDF #31-0965) and leucite ($KAlSi_2O_6$, PDF #38-1423), was observed, which indicated that the FA had undergone dissolution and reacted with a portion of the dehydrated $MgKPO_4$ phase. The feldspathoid minerals kalsilite and leucite are known to be thermally stable up to 1400 °C [30], which is encouraging from a fire performance perspective. A similar transition was previously observed in FA-derived geopolymers, where leucite was identified as the main crystalline product formed in K-aluminosilicate binders upon exposure to high temperature [31]. Other changes in the phase assemblage observed at this temperature included the formation of $K_3P_3O_7$ (#70-0048) and $Mg_2P_2O_7$ (PDF #32-0626). Hematite (Fe_2O_3, #33-0664) reflections identified at 1000 °C suggest that the Fe environments present in the glassy fraction of FA reorganised as a result of the FA reacting, which may be associated with the distinctive colour change shown in Figure 2.

3.3.2 GBFS/MKPC

At 20 °C in the GBFS/MKPC binder (Fig. 5), struvite-K was identified as the main binding phase, with unreacted MgO and a small reflection at 2θ = 31.3° assigned to åkermanite (Ca_2MgSiO_7, #76-0841), which is a crystalline phase present in the raw slag. The behaviour of GBFS/MKPC (Fig. 4) at 200 °C was similar to that of FA/MKPC (Fig. 4); again, no crystalline reflections were identified that could be associated with a dehydrated $KMgPO_4$ phase.

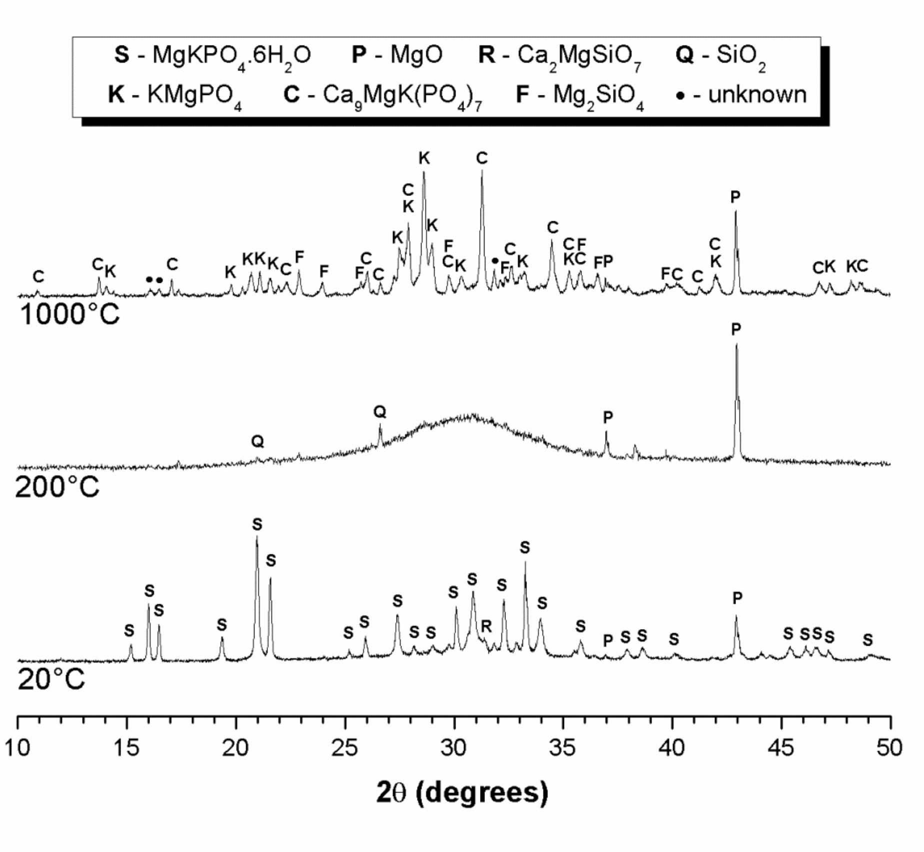

Fig. 5. X-ray diffraction patterns of GBFS/MKPC pastes exposed to temperatures of 20, 200 and 1000 °C.

As discussed above, it is postulated that $KMgPO_4$ is non-crystalline between 200 °C - 700 °C[25-27], as a result of dehydration of struvite-K. Diffuse scattering associated with the glassy slag fraction is reported between 15° < 2θ ≤ 35° [24], however the diffuse scattering in the 200 °C diffraction pattern was evident over a wider range (between 20° < 2θ ≤ 40°), suggesting that more than one amorphous phase could be present. The quartz identified at 200 °C is believed to be contamination from the cleaning media (sand) used during grinding.

At 1000 °C, the reflections assigned to $KMgPO_4$ (PDF #50-0149) emerged, suggesting that the long-range crystallographic order was restored. Forsterite (Mg_2SiO_4, PDF #34-0189) and a calcium magnesium potassium phosphate phase ($Ca_9MgK(PO_4)_7$, #45-0137) were also identified, which is indicative of GBFS reacting in the binder. Unlike the FA/MKPC binder at 1000 °C, no potassium aluminosilicate phases were observed, which suggested that the GBFS had not completely reacted at the temperature. As such, it is postulated further changes in the phase assemblage could occur at >1000 °C.

3.5 Scanning electron microscopy

Backscattered electron micrographs of FA/MKPC and GBFS/MKPC binders are shown in Figures 6 and 7; the appearance of the control samples at 20 °C (Figs. 6a and 7a) is typical for these binders as reported in the literature [12, 24]. It was observed in both systems that the main binding phase, struvite-K, formed a continuous phase that was interspersed with embedded large struvite-K crystallites. The large struvite-K crystals are known mainly to occur in systems prepared using boric acid to retard the setting reaction [32] this retardation provides sufficient time to allow large ordered crystallites to form within the adhesive binder [33]. The large struvite-K radial structures were highly cracked, which is a dehydration/desiccation artefact associated with sample preparation under vacuum for electron microscopy. In addition to struvite-K, spherical particles of varying sizes corresponding to FA particles (Fig. 6a) were observed, while angular light grey particles were found to correspond to unreacted GBFS (Fig. 7a). Unreacted periclase (determined in XRD assignments in Figs. 4 and 5) was identified as dark grey angular particles in both Figures 6a and 7a.

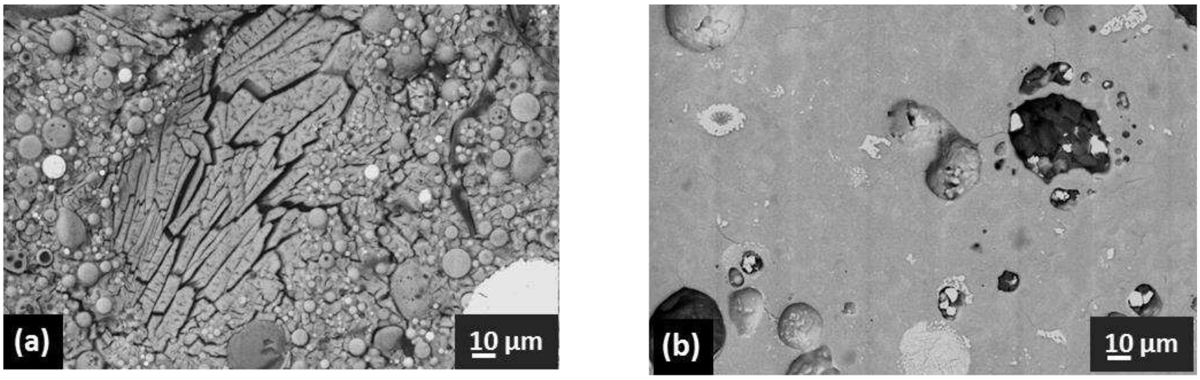

Fig. 6. SEM micrographs of FA/MKPC hardened pastes at (a) 20 °C and (b) 1000 °C.

In Figure 6, clear differences can be identified between the FA/MKPC binder microstructures at 20 °C and 1000 °C. Significant densification occurred after treatment at 1000 °C in the FA/MKPC sample; we postulate that this is a result of the glassy FA particles partially melting and reacting with the dehydrated $MgKPO_4$ phase. This sintering process resulted in a largely homogenous morphology as observed in Figure 6b, however, several discrete phases were observed (based on grey-scale differences) in the smooth binder. Several heterogeneous phases were also observed that appeared to be Fe-rich (we postulate this as brighter backscattered electron features are associated with heavier elements, of which Fe is the most appropriate in blended MKPC binders). The chemical reorganisation of the binder produced a ceramic-like microstructure, which is in good agreement with the new phases identified in the XRD patterns (Fig. 4) including kalsilite and leucite. This observation has also been highlighted in thermally treated fly ash geopolymers exposed to temperatures above 1200 °C [34]. The Fe present in the FA particles was observed to redistribute when compared to the 20 °C sample, where Fe was found to be associated with the bright spherical particles. At 1000 °C, the Fe was associated with hematite (confirmed in XRD analysis; Fig. 4).

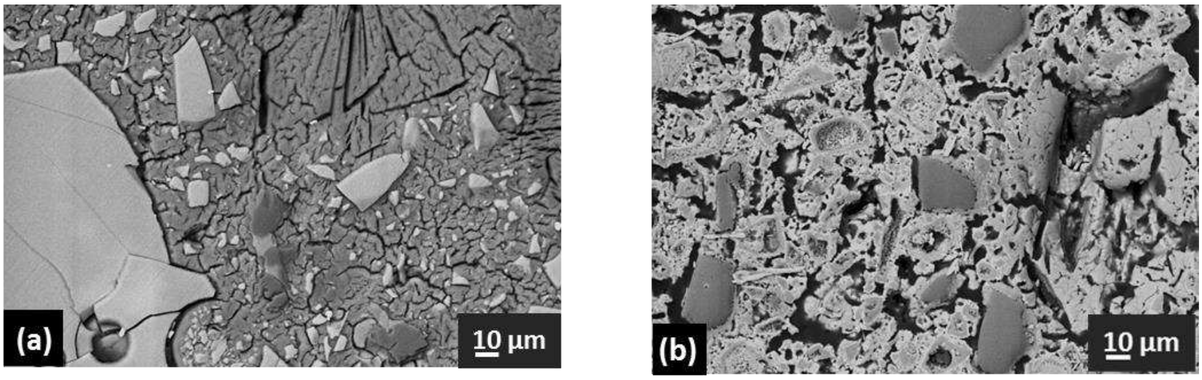

Fig. 7. SEM micrographs of GBFS/MKPC hardened pastes at (a) 20 °C and (b) 1000 °C.

Microstructural differences were observed in the GBFS/MKPC binder exposed to 1000 °C (Fig. 7b) compared to the 20 °C sample. The porosity (identified as the black areas) was observed to significantly increase, commensurate with the volumetric and mass changes reported in Table 3. A continuous phase was present at 1000 °C; this was associated with the dehydrated struvite-K phase, $MgKPO_4$, which was interspersed with unreacted periclase (dark grey angular particles). Despite the high temperature treatment, it is still possible to distinguish the shape of the relict GBFS particles within the binder matrix. A "reaction rim" was clearly apparent on these relict GBFS particles; this is associated with Ca dissolution leading to the formation of the $Ca_9MgK(PO_4)_7$ phase, as identified in X-ray diffraction analysis (Fig. 5).

4. CONCLUSIONS

The exposure of FA/MKPC and GBFS/MKPC binders to 200 °C resulted in the dehydration of $MgKPO_4{\cdot}6H_2O$ and consequent formation of non-crystalline $KMgPO_4$. At 1000 °C, several phases were identified in FA/MKPC that were indicative of reaction between FA and the dehydrated MKPC matrix, namely in the formation of a feldspathoid minerals kalsilite and leucite. This phase reorganisation resulted in a more homogenous microstructure when compared to the binder structure at 20 °C. After exposure to 1000 °C, the GBFS/MKPC binder developed a porous microstructure, which was associated with dehydrated $KMgPO_4$

matrix. A new crystalline phase, $Ca_9MgK(PO_4)_7$, was observed, which suggested the GBFS had started to react. However no Al or Si phases were observed, it is therefore postulated that this reaction was not yet complete. It is hypothesised that above 1000 °C, the GBFS/MKPC would undergo a conversion to a ceramic-like microstructure similar to that observed in the FA/MKPC binder. Although the FA/MKPC and GBFS/MKPC binders were significantly altered at high temperatures, they formed well-known stable products that resulted in no spalling and cracking of the samples. This suggests that these formulations could withstand the fire performance requirements associated with transport [22] and geological disposal [13] of nuclear wasteforms. Further work is currently underway to explore the phase assemblage and microstructure transitions at intermediary and higher temperatures to provide a better understanding of MKPC binders exposed to high temperature.

ACKNOWLEDGEMENTS

LJG is grateful to the Nuclear Decommissioning Authority for sponsorship, under supervision by the National Nuclear Laboratory. NCH wishes to acknowledge the Royal Academy of Engineering, the Nuclear Decommissioning Authority and EPSRC for funding support (EP/L014041/1). CLC is grateful to the University of Sheffield for the award of a Vice Chancellor's fellowship. This research was performed in part at the MIDAS Facility, at the University of Sheffield, which was established with support from the Department of Energy and Climate Change.

REFERENCES

1. F. Qiao, C. K. Chau, and Z. Li: 'Property evaluation of magnesium phosphate cement mortar as patch repair material', *Construction and Building Materials*, 2010, **24**(5), 695-700.
2. N. B. Milestone: 'Reactions in cement encapsulated nuclear wastes: need for toolbox of different cement types', *Advances in Applied Ceramics*, 2006, **105**(1), 13-20.

3. D. Singh, A. S. Wagh, J. C. Cunnane, and J. L. Mayberry: 'Chemically bonded phosphate ceramics for low-level mixed-waste stabilization', *Journal of Environmental Science and Health . Part A: Environmental Science and Engineering and Toxicology*, 1997, **32**(2), 527-541.

4. D. Singh, A. S. Wagh, M. Tlustochowicz, and S. Y. Jeong: 'Phosphate ceramic process for macroencapsulation and stabilization of low-level debris wastes', *Waste Management*, 1998, **18**(2), 135-143.

5. D. Singh, S. Y. Jeong, and K. Dwyer: 'Ceramicrete: a novel ceramic packaging system for spent-fuel transport and storage', Waste Management Conference, Tucson, AZ, USA, 2000.

6. D. Singh, V. R. Mandalika, S. J. Parulekar, and A. S. Wagh: 'Magnesium potassium phosphate ceramic for ^{99}Tc immobilization', *Journal of Nuclear Materials*, 2006, **348**(3), 272-282.

7. A. S. Wagh, S.-Y. Jeong, and D. Singh: 'Mercury stabilization in chemically bonded phosphate ceramics', American Ceramic Society San Antonio, TX, USA, 1997.

8. A. S. Wagh, R. Strain, S. Y. Jeong, D. Reed, T. Krause, and D. Singh: 'Stabilization of Rocky Flats Pu-contaminated ash within chemically bonded phosphate ceramics', *Journal of Nuclear Materials*, 1999, **265**(3), 295-307.

9. A. S. Wagh, M. D. Maloney, G. H. Thomson, and A. Antink: 'Investigations in ceramicrete stabilization of hanford tank wastes', Waste Management Conference, Tucson, AZ, USA, 2003.

10. J. H. Sharp, N. B. Milestone, J. Hill, and E. W. Miller: 'Cementitious systems for encapsulation of intermediate level waste', The 9th International Conference on Radioactive Waste Management and Environmental Remediation Oxford, England, 2003.

11. M. Hayes and I. H. Godfrey: 'Development of the use of alternative cements for the treatment of intermediate level waste', Waste Management Conference Tuscon, AZ, USA, 2007.

12. A. Covill, N. C. Hyatt, J. Hill, and N. C. Collier: 'Development of magnesium phosphate cements for encapsulation of radioactive waste', *Advances in Applied Ceramics*, 2011, **110**(3), 151-156.

13. Nuclear Decommissioning Authority: 'Geological Disposal: Waste package accident performance status report, NDA/RWMD/032', 2010.

14. Nuclear Decommissioning Authority: 'Waste package specification and guidance documentation; WPS/300/02, specification for 500 litre drum waste package', 2008.

15. U.S Department of Energy: 'Waste isolation pilot plant recovery plan, revision 0', 2014.

16. F. Delhomme, J. Ambroise, and A. Limam: 'Effects of high temperatures on mortar specimens containing Portland cement and GGBFS*', Materials and Structures*, 2012, **45**(11), 1685-1692.

17. D. Matesová, D. Bonen, and S. P. Shah: 'Factors affecting the resistance of cementitious materials at high temperatures and medium heating rates*', Materials and Structures*, 2006, **39**(4), 455-469.

18. W. D. Kingery: 'Fundamental study of phosphate bonding in refractories: I, literature review*', Journal of the American Ceramic Society*, 1950, **33**(8), 239-241.

19. R. W. Limes and D. Ponzani: 'Basic refractory compositions for intermediate temperature zones*',* Patent, 3, 285, 758, United States Patent Office, USA, 1966.

20. R. W. Limes and R. O. Russell: 'Process for preparing fast-setting aggregate compositions and products for low porosity produced therewith*',* Patent, 3,879,209, United States Patent Office, USA, 1975.

21. L. J. Gardner, C. L. Corkhill, S. A. Bernal, N. C. Collier, J. L. Provis, and N. C. Hyatt: 'The effect of water content on blended magnesium potassium phosphate cement binders for radioactive waste encapsulation*', manuscript in preparation*, 2015.

22. International Atomic Energy Agency: 'Regulations for the safe transport of radioactive material; specific safety requirements; 2012 edition, Vienna', 2012.

23. S. Zhang, H. Shi, S. Huang, and P. Zhang: 'Dehydration characteristics of struvite-K pertaining to magnesium potassium phosphate cement system in non-isothermal condition*', Journal of Thermal Analysis and Calorimetry*, 2013, **111**, 35-40.

24. L. J. Gardner, S. A. Bernal, S. A. Walling, C. L. Corkhill, J. L. Provis, and N. C. Hyatt: 'Characterisation of magnesium potassium phosphate cements blended with fly ash and blast furnace slag*', Cement and Concrete Research*, 2015, **74**, 78-87.

25. R. Neiman and A. C. Sarma: 'Setting and thermal reactions of phosphate investments', *Journal of Dental Research*, 1980, **59**(9), 1478-1485.

26. A. K. Sarkar: 'Hydration/dehydration characteristics of struvite and dittmarite pertaining to magnesium ammonium phosphate cement systems', *Journal of Materials Science*, 1991, **26**(9), 2514-2518.

27. B. E. I. Abdelrazig and J. H. Sharp: 'Phase changes on heating ammonium magnesium phosphate hydrates', *Thermochimica Acta*, 1988, **129**(2), 197-215.

28. S. Graeser, W. Postl, H.-P. Bojar, P. Berlepsch, T. Armbruster, T. Raber, K. Ettinger, and F. Walter: 'Struvite-(K), $KMgPO_4{\cdot}6H_2O$, the potassium equivalent of struvite – a new mineral', *European Journal of Mineralogy*, 2008, **20**(4), 629-633.

29. M. Mathew and L. W. Schroeder: 'Crystal structure of a struvite analogue, $MgKPO_4{\cdot}6H_2O$', *Acta Crystallographica: Section B Structural Crystallography and Crystal Chemistry*, 1979, **35**(1), 11-13.

30. V. F. F. Barbosa and K. J. D. MacKenzie: 'Synthesis and thermal behaviour of potassium sialate geopolymers', *Materials Letters*, 2003, **57**(9–10), 1477-1482.

31. T. Bakharev: 'Thermal behaviour of geopolymers prepared using class F fly ash and elevated temperature curing', *Cement and Concrete Research*, 2006, **36**, 1134-1147.

32. D. A. Hall, R. Stevens, and B. El-Jazairi: 'The effect of retarders on the microstructure and mechanical properties of magnesia–phosphate cement mortar', *Cement and Concrete Research*, 2001, **31**(3), 455-465.

33. A. D. Wilson and J. W. Nicholson: 'Acid-base cements: their biomedical and industrial applications'; 1993, Cambridge University Press.

34. T. Bakharev: 'Thermal behaviour of geopolymers prepared using class F fly ash and elevated temperature curing', *Cement and Concrete Research*, 2006, **36**(6), 1134-1147.

FIGURE CAPTIONS

Fig. 1. Fire performance thermal treatment programme.

Fig. 2. Photographs of a) FA/MKPC and b) GBFS/MKPC hardened pastes exposed to temperatures of 20, 200 and 1000 °C. The samples are; 14 mm diameter (± 0.6 mm) and 10 mm height (± 0.5 mm).

Fig. 3. a) TGA and b) DTG data for FA/MKPC and GBFS/MKPC pastes after 7 days curing.

Fig. 4. X-ray diffraction patterns of FA/MKPC pastes exposed to temperatures of 20, 200 and 1000 °C.

Fig. 4. X-ray diffraction patterns of GBFS/MKPC pastes exposed to temperatures of 20, 200 and 1000 °C.

Fig. 6. SEM micrographs of FA/MKPC hardened pastes at (a) 20 °C and (b) 1000 °C.

Fig. 7. SEM micrographs of GBFS/MKPC hardened pastes at (a) 20 °C and (b) 1000 °C.